



# A crop water stress index based internet of things decision support system for precision irrigation of wine grape<sup>☆</sup>

Bradley A. King<sup>a,\*</sup>, Krista C. Shellie<sup>b</sup>

<sup>a</sup> Research Agricultural Engineer, USDA ARS Northwest Irrigation and Soils Research Laboratory, 3793N 3600 E, Kimberly, ID 83341, USA

<sup>b</sup> Research Horticulturalist (retired), USDA-ARS Horticultural Crops Research Unit, Corvallis, OR 97330, USA

## ARTICLE INFO

Editor: Dr Spyros Fountas

### Keywords:

Irrigation  
Wine grape  
Crop water stress index  
Edge computing  
Decision support system  
Internet of Things

## ABSTRACT

The goal of irrigation for wine grape grown in arid or semiarid regions is to sustain vine survival and to optimize berry attributes for quality wine production. Precision irrigation of wine grape is impeded by the lack of a smart, decision support system (DSS) to remotely monitor vine water status. The objectives of this study were to: develop and field test an Internet of Things (IoT) DSS system for precision irrigation of wine grape. The IoT system was comprised of a suite of *in situ* sensors used to monitor real-time weather conditions, grapevine canopy temperature, soil moisture, and irrigation amount. Sensor data were collected and stored on a field deployed data logger that calculated a daily thermal Crop Water Stress Index (CWSI) for grapevine using a neural network model with real-time sensor data model inputs. The data logger also hosted, via a cellular modem, webpages showing a running, 12-day history of daily CWSI, fraction of available soil moisture (fASW), irrigation amount, and other sensor data. The webpages were accessible to vineyard managers via cell phone or computer. The CWSI based IoT DDS system was installed at two small acreage, commercial estate vineyards in southwestern Idaho USA over four growing seasons. At each vineyard site, the DSS was used daily by the vineyard irrigation manager to schedule irrigation events. Neither vineyard manager used any other quantitative vine water status monitoring tool for irrigation management decisions. The midday leaf water potential (LWP) of grapevines was routinely measured by research project personnel. Data collected over the study period at each vineyard showed a significant ( $p < 0.001$ ) correlation with LWP and fASW, providing evidence that, under the conditions of this study, the daily CWSI based IoT provided automated, remote monitoring of vine water status. Both vineyard managers reported daily use of the DSS for irrigation scheduling decisions. Over the four-year study, each vineyard manager was able to maintain consistent seasonal average CWSI daily values and irrigation application amounts, despite yearly differences in climatic conditions. The results of this study demonstrate that a CWSI based IoT DSS can be used for precision irrigation of wine grape in a commercial vineyard under semiarid growing conditions. The CWSI based IoT DSS used a unique combination of neural network modeling, edge computing, and IoT for real-time vine water stress monitoring for precision irrigation.

## 1. Introduction

Irrigation management of most field crops aims to avoid plant water stress and maximize yield by supplying water to fully meet crop evapotranspiration (ET<sub>c</sub>). However, in wine grape (*Vitis vinifera* L.), fruit quality attributes are prioritized over yield as a production goal, and development of the berry and vine canopy are related to vine water status throughout the growing season [1,2]. For example, mild vine water stress between veraison (berry softening) and harvest is desirable

to prevent berry splitting or dilution of flavors or sugars and to slow canopy growth in preparation for winter dormancy. Inducing vine water stress through deficit irrigation has also been shown to increase vine water use efficiency [3–5].

Water resources in the western U.S. are experiencing unprecedented competitive demand from irrigated agriculture, growing urban populations, and environmental and ecosystem restoration. Groundwater levels in many areas have steadily decreased from historic levels and ground water use is approaching an unsustainable level. In addition, the

<sup>☆</sup> Mention of company or trade names is for description only and does not imply endorsement by the USDA. The USDA is an equal opportunity provider and employer.

\* Corresponding author.

E-mail address: [brad.king@usda.gov](mailto:brad.king@usda.gov) (B.A. King).

<https://doi.org/10.1016/j.atech.2023.100202>

Received 30 March 2022; Received in revised form 16 February 2023; Accepted 17 February 2023

Available online 19 February 2023

2772-3755/Published by Elsevier B.V. This is an open access article under the CC BY license (<http://creativecommons.org/licenses/by/4.0/>).

western US is experiencing the worst megadrought since 800 CE [6] leading to historically low water levels in many of the regions water reservoirs. Warmer winter temperatures due to climate change are predicted to reduce future mountain snowpack, which is the source of early irrigation developments in much of the western U.S. The growing demand on surface and groundwater resources combined with climate change necessitates increased water resource stewardship and crop water productivity to meet food and fiber needs of a growing population.

Wine grape production in semiarid regions of the Pacific northwestern U.S. is well established but relies on irrigation during the growing season for vine growth, survival, and economically viable yield. Optimum management of irrigation requires routine direct or indirect monitoring of vine water status [7]. Indirect methods for accessing plant water status include soil water content or soil water potential measurement and atmospheric-based methods [7,8]. Soil water monitoring is a widely accepted tool for estimating crop water needs for field crops but in the case of vineyards there are several disadvantages. These include spatial variability in soil characteristics and 3-dimensional soil wetting patterns from drip irrigation leading to the need to install several sensors, which complicates information management and increases cost. Additionally, there is a lack of established thresholds for determining vine water status and severity [7]. Atmospheric based methods include Bowen ratio energy balance and eddy covariance to determine  $ET_c$  and infer plant water status by comparing measured  $ET_c$  to estimated non-water stressed  $ET_c$ . These techniques require expensive sensors, skilled technical knowledge, and large uniform upwind fetch, especially for eddy covariance, which make them unsuited for small commercial vineyard water management purposes [7]. A more detailed discussion of indirect methods is provided by Rienth and Scholasch [8].

Direct (plant-based) methods for determining plant water status rely on measurements of physical plant variables. Unlike indirect methods, plant-based methods use the plant as a biosensor in a soil-plant-atmosphere continuum. Conventional direct methods include leaf or stem water potential, visual observation, stomatal conductance or photosynthesis, sap flow, trunk diameter and leaf turgor pressure [7,9]. Midday stem or leaf water potential (LWP) is the most commonly accepted direct measurement of vine water status [10] and critical upper and lower water stress thresholds have been established [7], making it an effective tool for deficit irrigation management. The primary disadvantages of LWP are the limited time of day for measurement, the need for repeated measurements due to plant variability, and a need for several equipped and trained personnel to cover a vineyard. Visual observation is based on the visual growth characteristics of the apical meristem or apex of vines, tendrils, and leaf orientation of numerous vines [1,8]. The drawbacks of this method include low sensitivity to moderate water stress, time lag between water stress and visual observation, and the cost of trained personnel to cover a vineyard. Stomatal conductance measures the ease of passage of  $CO_2$  or water vapor through the stomata and is a good indicator of plant response to water stress because it changes with atmospheric demand and soil water status. It has been shown to indicate the degree of vine water stress but varies with timing of measurement and leaf canopy location [7]. The primary disadvantages are the cost of the equipment, constant need for calibration, technical skill to operate. Sap flow, trunk diameter and leaf turgor are direct measures that have been shown to be indicators of plant water stress. However, they have not been widely adopted in regional commercial vineyards but have the advantage of being automated, which facilitates integration into a deficit irrigation management program. Detailed descriptions of other direct methods and their respective advantages and disadvantages are provided by [7–9].

Plant canopy temperature increases when solar radiation is absorbed and cools when water is evaporated (transpiration) within the leaf structure. A water-stressed plant canopy will reduce transpiration and have a higher temperature than a non-stressed canopy [11,12]. This physical plant response to water stress makes canopy temperature measurement a viable direct method for assessing plant water status.

Infrared radiometers have been used to measure plant canopy temperature under research field conditions to estimate evapotranspiration and drought stress in many crops [13–15], including grape [16–21]. Infrared thermometry is nondestructive, can be measured continuously, can be stationary or mounted on mobile platforms for spatial and temporal monitoring [9,20–22], and can be less expensive [23] than soil water sensing. Canopy temperature is related to plant water status, but it also depends upon solar radiation ( $R_s$ ), air temperature ( $T_a$ ), humidity (RH), and wind speed (WS) among other things.

A method of using canopy temperature to calculate a CWSI for irrigation scheduling was proposed over 40 years ago by Idso et al. [15] and Jackson et al. [14]. The CWSI normalizes measured canopy temperature relative to reference threshold canopy temperatures for a well-watered vine ( $T_{LL}$ ) and a water stressed, non-transpiring vine ( $T_{UL}$ ) under identical weather conditions, resulting in an empirical CWSI value between, 0 (no water stress) and 1 (maximum water stress). Unfortunately, the need for  $T_{LL}$  and  $T_{UL}$  reference temperatures under identical weather conditions has limited the use of a CWSI to research scale studies and precluded its adoption on a commercial scale [9]. Alternatives to actual measurement of crop reference temperatures have been investigated, such as artificial wet and dry surfaces [16,24–29] and physical and empirical models [14,26,30–33] to predict reference temperatures. The required maintenance of an artificial surface has limited use on a commercial scale, leaving physical or empirical models as the most logical choice. King et al. [33] used measured temperatures of non-water stressed wine grape canopies to develop data driven models (neural network, regression) to estimate  $T_{LL}$ . The models were used to calculate CWSI values for research plots of Malbec grapes vines that were differentially irrigated to induce differing severities of vine water stress [19] and validated by comparing, over a 5-year period, CWSI values with LWP and fASW. The CWSI calculated using model predicted reference temperatures was well correlated with LWP ( $R^2 = 0.54$ ) and fASW ( $R^2 = 0.71$ ). When CWSI values were used to trigger 28 mm irrigation events, CWSI values increased, LWP became more negative, seasonal water application decreased, and grape cluster weight decreased. These results demonstrated that a CWSI could be used as an effective irrigation scheduling tool for wine grape.

Irrigation scheduling based on canopy temperature has not been adopted on a commercial scale by vineyard irrigation managers in semiarid regions of northwestern U.S. as evident by the lack of commercial systems supporting the application. The objectives of this study were to: develop a CWSI based IoT DSS for precision irrigation of wine grape under semiarid conditions; field test the CWSI based IoT DSS in two, small acreage commercial estate vineyards over four growing seasons; validate the IoT derived CWSI values by statistical correlation with LWP and fASW at each vineyard site; and evaluate vineyard manager annual consistency in irrigation scheduling. Vineyard irrigation managers were allowed to freely decide if they wanted to use the CWSI based IoT DSS for irrigation scheduling. Consistency of plant water stress and irrigation application across multiple years was used to gauge success of the CWSI based IoT DSS system for irrigation scheduling as implemented by the vineyard manager.

## 2. Methods and materials

### 2.1. Field study site characteristics

This study was conducted on two small (< 7 ha) family owned and operated commercial vineyards in southwestern Idaho USA over a four-year period (2017–2020). Both operations were estate vineyards in that they have associated wineries that produce branded commercial wines. The vineyard sites were located within 30 km of each other but differed in their soil characteristics and soil water holding capacities. The soil at vineyard-A (V-A) was a Greenleaf-Owyhee silt loam (fine-silty, mixed, superactive, mesic Xeric Calciargids) characterized as very deep well drained with moderately slow permeability and an available water

capacity of  $0.2 \text{ cm}^{-1}$  (USDA Web Soil Survey). Vineyard-B (V-B) was located adjacent to an ancient volcanic vent that had been subjected to limited volcanic rock mining. The vineyard site was reclaimed using surrounding soil and original overburden to cover exposed rock resulting in a highly disturbed soil profile. The natural soils at the site were Turbifyll fine sandy loam (coarse-loamy, mixed, superactive, calcareous, mesic Xeric Torriorthents) and Jacquith loamy fine sand (Sandy, mixed, mesic Xerptic Haplodurids), both of which are moderately deep and well drained in their natural state with moderately rapid permeability. Available water capacity of the Turbifyll fine sandy loam and Jacquith loamy fine sand were  $0.12$  and  $0.07 \text{ cm}^{-1}$ , respectively (USDA Web Soil Survey).

Vines in both vineyards were grown with double trunks on a vertically shoot positioned, two-wire trellis system with moveable catch wires. The vines were trained to bilateral cordons and spur-pruned annually to approximately  $16 \text{ buds m}^{-1}$  of cordon. Row by vine spacing was  $2.7 \text{ m} \times 1.8 \text{ m}$  at V-A and  $2.7 \text{ m} \times 1.5 \text{ m}$  at V-B.

Irrigation at both sites was applied using drip irrigation tubing suspended about  $30 \text{ cm}$  above ground in the vine row. Drip emitter spacing was  $76 \text{ cm}$  with a flow rate of  $3.8 \text{ L hr}^{-1}$  at V-A and  $61 \text{ cm}$  with a flow rate of  $1.9 \text{ L hr}^{-1}$  at V-B. The wine grape cultivar evaluated at V-A was Chardonnay (2017–2020) and the cultivars at V-B were Malbec (2017–2019) and Cabernet Sauvignon (2020).

## 2.2. Field measurements and instrumentation hardware and software

Canopy temperature was measured using wired infrared radiometers (SI-121, Apogee Instruments, Logan, Utah) with a  $36^\circ$  field of view. The radiometers were placed along a single vine row to prevent potential damage to sensor cables from vineyard equipment. In each vineyard, two (2017, 2018, 2019) or four (2020) radiometers were installed per cultivar. Radiometer cable lengths were  $30 \text{ m}$  allowing a maximum distance of  $60 \text{ m}$  between radiometers within a vine row. The radiometers were installed on vines with representative canopy size and positioned approximately  $15$  to  $30 \text{ cm}$  above fully expanded leaves located at the top of the vine canopy. Radiometers were pointed northeasterly at approximately  $45^\circ$  from nadir, with the sensor view aimed at the center of solar noon sunlit leaves. The temperature sensing area of vine canopy was approximately  $10$  to  $20 \text{ cm}$  in diameter and received full sunlight exposure during midday. The possibility of background bare soil visibility was limited by multiple leaf layers within the canopy below the measured canopy location. The infrared radiometer sensor view was periodically adjusted as necessary to ensure that the field of view concentrated on sunlit leaves near the top of the canopy. The infrared radiometers were installed after fruit set, usually mid to late June. Solar radiation ( $R_s$ ) (SP-110 pyranometer, Apogee Instruments, Logan, UT), air temperature ( $T_a$ ), relative humidity (RH) (HMP50 temperature and humidity probe, Campbell Scientific, Logan, UT), and wind speed (WS) (034B, Met One Instruments, Grants Pass, Ore.) were measured in each vineyard at a height of  $2.5 \text{ m}$ . Canopy temperature and weather parameters were measured every minute and recorded as  $15 \text{ min}$  averages on a datalogger (CR6, Campbell Scientific, Logan, UT). The weather sensors and data logger were installed in the same vine row and located midway between the infrared temperature sensors. The equipment was removed at harvest, usually mid to late September. A  $1.2 \text{ m}$  soil moisture sensor (Drill and Drop, SenTek Sensor Technologies, Stepney, SA) was installed in the vine row within  $3 \text{ m}$  of the data logger and within  $20 \text{ cm}$  of an irrigation drip line emitter. Soil moisture was recorded every  $30 \text{ min}$  measured at  $10 \text{ cm}$  depth increments to a depth of  $1.2 \text{ m}$ . In 2017 and 2018, a tipping bucket rain gage (RainWise, Boothwyn, PA) was placed under an drip line irrigation emitter to record cumulative irrigation application amount. The rain gage was connected to the data logger and total emitter water application was recorded in  $15 \text{ min}$  and  $24 \text{ hr}$  increments. In 2019 and 2020 a flow meter (36MP.75RG.1, Netafim Irrigation, Inc., Fresno, CA) was installed in the irrigation drip line and connected to the data logger. Flow rate was recorded in  $15 \text{ min}$

increments.

The field data logger was equipped with a machine-to-machine cellular modem (RavenXTA CDMA or RV50 Sierra wireless AirLink, Campbell Scientific Inc., Logan, UT) to provide real-time access to the sensor data using commercial software. Study personnel accessed sensor data using datalogger management software (LoggerNet 4.5, Campbell Scientific Inc., Logan, UT). Vineyard managers were provided real-time sensor data access through a website. The website was hosted on the field data logger. Data logger webpage publishing software (RTCM Pro Development 4.3.3.6, Campbell Scientific Inc., Logan, UT) was used to design and publish the webpage on the data logger. The website was accessible using either a personal computer or a smart phone. The website provided graphical pages with running 12-day histories of daily CWSI, soil water content at each depth increment, fASW, daily irrigation depth, and latest 15-min averaged weather data, each on a separate webpage. The website was available between the hours of 6:00 to 22:00 MDT. The cell phone modem was powered down overnight to conserve battery power and to reset the modem in case of intruder hacking and malware. The data logger battery was charged using a  $20 \text{ W}$  solar panel.

Midday LWP was measured at 7-to-10-day intervals in both vineyards in each year of the study to verify vine water status and to investigate its correlation with daily CWSI. LWP was measured between 13:00 and 15:00 MDT on two fully expanded, sunlit leaves from vines adjacent to each installed infrared radiometer using a pressure chamber (model 610, PMS Instrument Co., Albany, OR) as described by Levin et al. [10,34].

## 2.3. Calculated webpage values

Information shown on webpages hosted by the field data logger was based on several calculations performed by datalogger software using measured sensor values. The calculated values included daily CWSI, fASW, and daily irrigation depth. Daily CWSI was calculated as the average 15-min CWSI between 13:00 and 15:00 MST, which corresponded to  $-1$  to  $+1.5 \text{ hr}$  of solar noon. The 15-min CWSI was calculated using the empirical equation developed by Idso et al. [15] as:

$$CWSI = \frac{(T_c - T_{LL})}{(T_{UL} - T_{LL})} \quad (1)$$

where  $T_c$  is measured canopy temperature of fully sunlit leaves ( $^\circ\text{C}$ ). The  $T_{LL}$  reference temperature ( $^\circ\text{C}$ ) was estimated using cultivar specific neural network models [32]. Inputs to the neural network models were 15-minute averaged values of measured  $R_s$ ,  $T_a$ , RH and WS. The  $T_{UL}$  reference temperature ( $^\circ\text{C}$ ) was estimated using the energy balance-based equation of [14] as:

$$T_{UL} - T_a = \frac{r_a R_n}{\rho c_p} \quad (2)$$

where  $r_a$  is aerodynamic resistance ( $\text{s m}^{-1}$ ),  $R_n$  is net radiation ( $\text{W m}^{-2}$ ),  $c_p$  is heat capacity of air ( $\text{J kg}^{-1} \text{ } ^\circ\text{C}^{-1}$ ), and  $\rho$  is density of air ( $\text{kg m}^{-3}$ ). Aerodynamic resistance was estimated using the approach of [30] as described by [33] using the same cultivar specific data sets for well-watered wine grapes in southwestern Idaho. Values used for  $r_a$  were  $16.8 \text{ s m}^{-1}$  for Malbec and  $21 \text{ s m}^{-1}$  for Chardonnay and Cabernet Sauvignon. Net radiation was estimated as  $R_n = 0.9R_s - 60$  [33].

The fASW for a given soil profile depth was calculated as:

$$fASW = \frac{\sum_{i=1}^n \frac{(\theta_i - \theta_{pwpi})}{(\theta_{fci} - \theta_{pwpi})}}{n} \quad (3)$$

where  $\theta_i$  is measured volumetric soil water content for depth  $i$ ,  $\theta_{pwpi}$  is estimated volumetric soil water content at permanent wilting point for depth  $i$ ,  $\theta_{fci}$  is estimated volumetric soil water content at field capacity at depth  $i$ , and  $n$  is the number of  $10 \text{ cm}$  soil water content measurement depths considered. Field capacity for each soil depth was estimated as

the maximum soil water content measured 24 h after an irrigation event or soil water content at the beginning of the season for depths below the irrigation wetting front. Permanent wilting point (PWP) for each soil depth was estimated as 50% of field capacity (FC) or minimum soil water content measured. Values for  $\theta_{fc}$  and  $\theta_{pwp}$  were continually adjusted during the beginning of the season as soil water content measurements were collected. Three values of fASW were presented in the webpage: 0 to 60 cm, 0 to 90 cm, and 0 to 120 cm. Values shown in the webpages were expressed in English units as they were designed for use by vineyard managers located in the U.S.

Daily irrigation depth was calculated as the volume of water applied between 0:00 and 24:00 MDT divided by the drip irrigation lateral length represented and vine row spacing. In the case of rain gauges, the volume of water measured by the rain gage was divided by the emitter spacing and vine row spacing. In the case of flow meters, the daily volume of water applied was calculated by summing the flow rate in each 15 min interval multiplied by the time interval. The volume of water was divided by lateral length downstream of the flow meter and vine row spacing. The calculated irrigation depth was presented in the English unit of inches.

#### 2.4. Irrigation DSS vineyard manager accessible webpages

The irrigation DSS was comprised of six separate webpages that displayed daily CWSI values (Fig. 1), soil moisture at depth of 0 to 60 cm (0 - 24 in) (Fig. 2), soil moisture at a depth of 70 to 120 cm (28 - 48 in) (Fig. 3), fASW at three soil depths (Fig. 4), irrigation amount (Fig. 5), and weather (Fig. 6). The webpages showing CWSI, soil water content (%) and fASW displayed data as a running 12-day history. Each webpage had a top menu showing all available webpages. CWSI values were graphed independently for each infrared radiometer and as the average value of all radiometers. An example of the main webpage at site V-B for 13 August through 25 August 2020 is shown in Fig. 1. Soil volumetric water content (%) was graphed independently at depth increments of 10 cm (4 inches) (Figs. 2,3). fASW (Fig. 4) was graphed independently for soil depths 0 to 60 cm (0 - 24 in), 0 to 90 cm (1 - 36 in), and 0 - 120 cm (0 - 48 in). Daily irrigation amounts (Fig. 5) represent water applied between 0:00 and 24:00 MDT. Figs. 1–5 show data for V-B from 13 August through 23 August 2020. Weather conditions in each vineyard (Fig. 6) were displayed as the most current 15-min average value for  $T_a$ , RH, WS, and wind direction. For ease of use, the values for  $T_a$  and RH were displayed graphically as well as numerically.

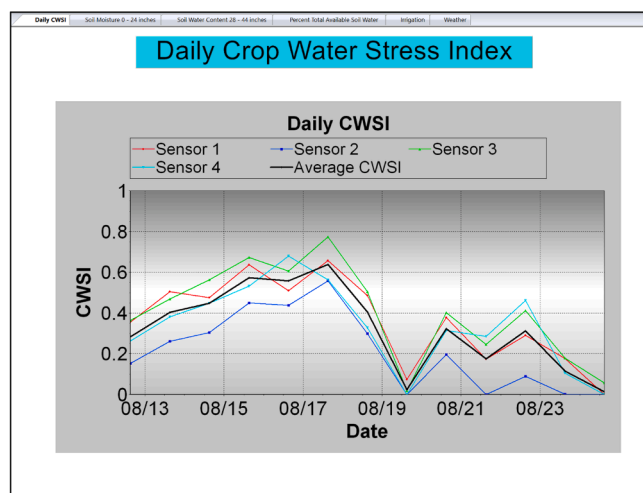


Fig. 1. Example main webpage showing daily crop water stress index (CWSI) for a 12-day period during 2020 at V-B.

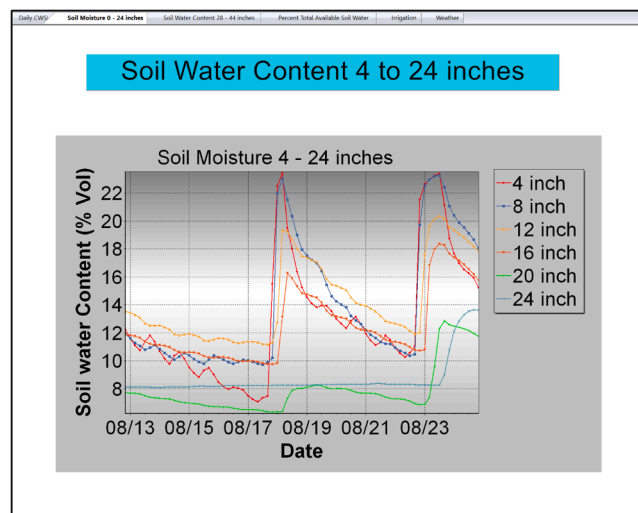


Fig. 2. Example webpage showing volumetric soil water content for 10 to 60 cm (4 to 24 inch) depths for a 12-day period during 2020 at V-B.

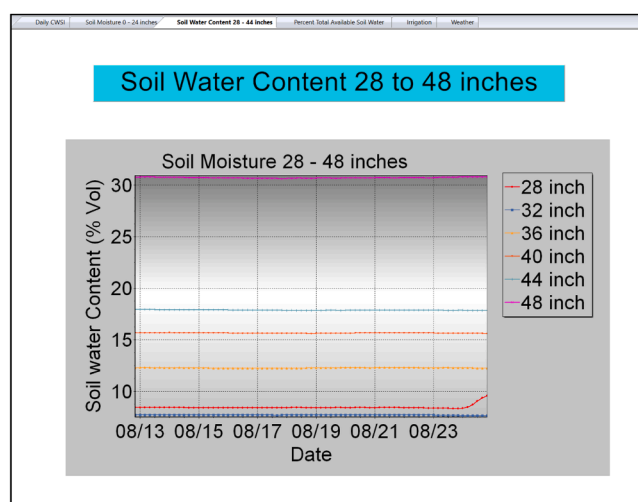


Fig. 3. Example webpage showing volumetric soil water content for 70 to 120 cm (28 to 48 inch) depths for a 12-day period during 2020 at V-B.

#### 2.5. Data analysis

Linear and multiple regression were conducted using Microsoft Excel data analysis tools. Graphical, linear, and multiple linear regression and variance analysis were used to quantify and evaluate relationships between variables. Regression line significance was evaluated using ANOVA ( $p < 0.05$ ). Neural network model development was performed using the MATLAB Neural Network Toolbox (MathWorks, Natick, Mass.) [33]. Graphs were generated using Sigmaplot 14 (Systat Software, San Jose, CA).

### 3. Results

#### 3.1. Climatic conditions

Climatic conditions during the four-year study relative to 20-yr (1996–2016) averages are summarized in Table 1. The climatic conditions during the four study years were generally within one standard deviation of the 20-yr mean with a few exceptions. Alfalfa-based reference evapotranspiration was greatest in 2018 and exceeded the 20-yr mean by more than one standard deviation. The combination of high



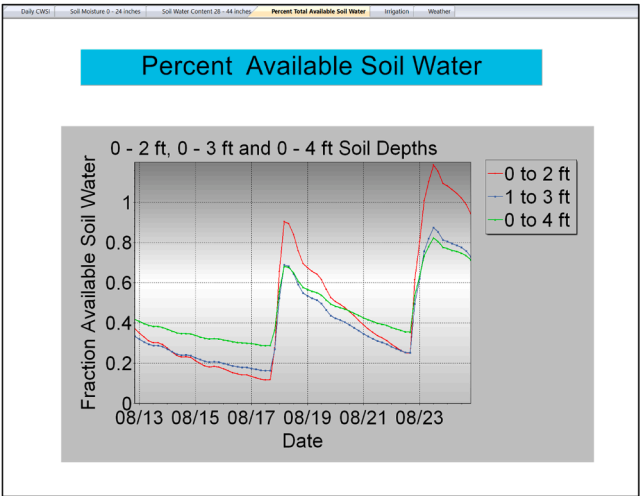


Fig. 4. Example webpage showing estimated fraction of available soil water for three soil profile depths for a 12-day period during 2020 at V-B; 0 to 60 cm (0 to 14 inch), 0 to 90 cm (0 to 36 inch), and 0 to 120 cm (0 to 48 inch).

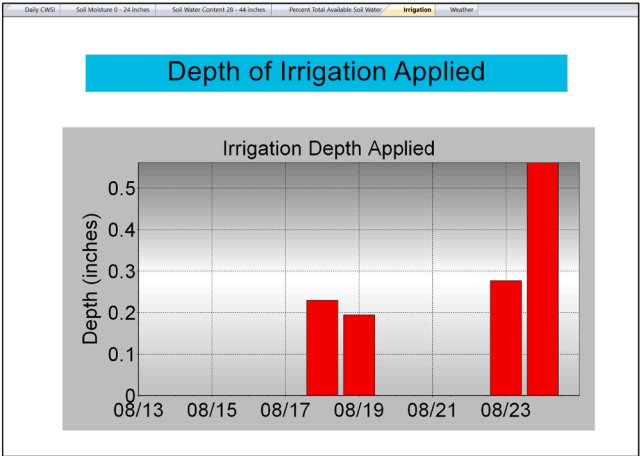


Fig. 5. Example webpage showing daily irrigation applied over a 12-day period during 2020 at V-B.

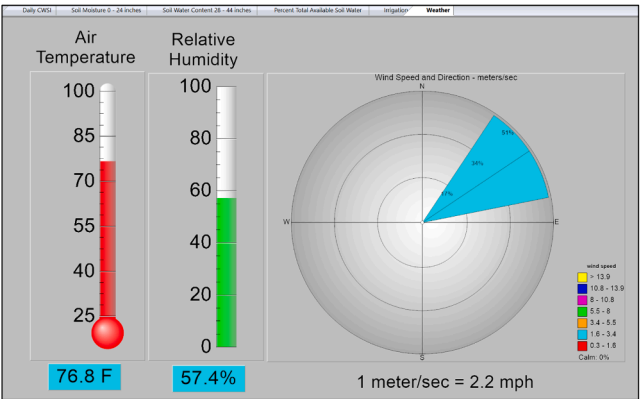


Fig. 6. Example of webpage displaying the latest 15-minute average measured values of air temperature, relative humidity, and windspeed and direction.

mean air temperature and daily solar radiation, and low mean relative humidity and April through September precipitation resulted in the high reference evapotranspiration in 2018. October through March

Table 1

Climatic conditions at weather station (PMAI, [www.usbr.gov/pn/agrimet/](http://www.usbr.gov/pn/agrimet/)) nearest (within 30 km) to study sites. Mean daily air temperature, relative humidity, and solar radiation, cumulative precipitation, alfalfa-based reference evapotranspiration, days air temperature > 35 °C, and growing degree days between 1 April through 30 September, and cumulative precipitation between 1 October and 31 March and 1 April to 30 September in each study year. The 20-yr averages (1996–2016) and standard deviations are also shown.

Parameters	2017	2018	2019	2020	1996–2016 Mean ± Std Dev
Mean air temperature ( °C)	18.9	19.0	18.3	18.1	18.4 ± 0.8
Days air temperature > 35 °C	39	33	27	23	29 ± 11
Mean relative humidity (%)	52.1	47.8	55.3	52.5	50.5 ± 3.3
Mean daily solar radiation (MJ m <sup>-2</sup> d <sup>-1</sup> )	23.2	24.3	23.5	23.7	23.9 ± 0.8
Alfalfa-based reference evapotranspiration (mm)	1192	1264	1164	1172	1158 ± 67
Precipitation Oct – Mar (mm)	239	102	168	121	128 ± 40
Precipitation Apr – Sept (mm)	77	50	142	201	80 ± 30
Growing-degree days ( °C) <sup>a</sup>	1639	1683	1584	1601	1595 ± 99

<sup>a</sup>Growing-degree days were calculated from daily maximum and minimum temperature with no upper limit and a base temperature of 10 °C.

precipitation was greatest in 2017 and exceeded one standard deviation of the 20-yr mean. April through September precipitation in 2019 and 2020 exceeded one standard deviation of the 20-yr mean. Growing-degree days was greatest in 2018, coinciding with highest mean daily air temperature and high reference evapotranspiration.

### 3.2. Relationship between measures of vine water stress

Linear relationships between plant water stress measures fASW, LWP, and CWSI at each vineyard for the four study years combined are summarized in Fig. 7. All the linear relationships between the water stress measures were statistically significant ( $p < 0.001$ ). The linear relationships between fASW versus LWP and daily CWSI versus LWP had similar  $R^2$  values for both vineyards. The linear relationship between fASW and CWSI at V-B had a much greater  $R^2$  than for V-A (0.58vs 0.32). Variability in the fASW vs CWSI data was similar between the vineyards, but daily CWSI spanned a greater range at V-B resulting in a greater  $R^2$ . The greatest data variability occurred between daily CWSI and LWP for both vineyards. The greater variability is likely due to CWSI and LWP responding differently to Ta, RS, RH and WS.

### 3.3. Relationship between seasonal CWSI and seasonal irrigation amounts

The seasonal average values for daily CWSI and the cumulative amount of irrigation applied between 1 July and 15 September in each study year at each vineyard are shown in Table 2. The seasonal average daily CWSI values for each vineyard were largely consistent over the four-year study. Seasonal daily CWSI values were higher for V-B as the vineyard manager preferred higher plant water stress than the manager of V-A. The higher daily CWSI value at V-B was also higher because it would rapidly increase a couple days after an irrigation event due to the low water holding capacity of the sandy soil.

## 4. Discussion

### 4.1. Irrigation DSS vineyard manager accessible webpages

An example of the irrigation DSS running 12-day history and weather webpage is presented for V-B for 13 to 23 August 2020 (Figs. 1–6). An irrigation event, starting the evening of 18 August 2020, increased soil water content to a depth of 60 cm (24 inches) (Fig. 2) and decreased the daily CWSI to near zero (Fig. 1). An irrigation event starting on the evening of 23 August increased soil water content to a depth 70 cm (28

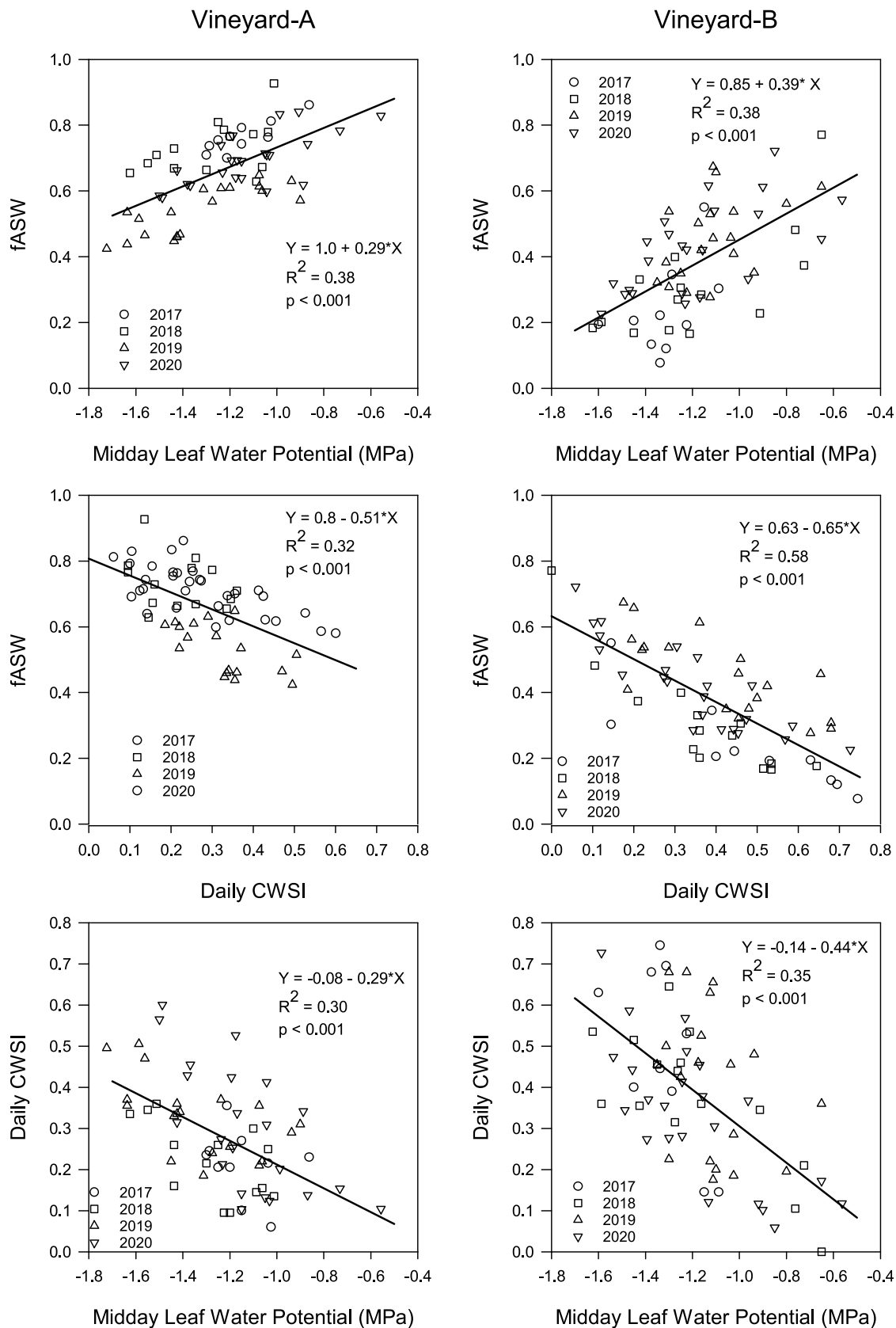


**Fig. 7.** Relationships between average daily CWSI, fraction of available soil water (fASW) in 0 to 120 cm soil profile, and midday leaf water potential (LWP) for the four study years at V-A (left graphs) and V-B (right graphs).

**Table 2**  
Average daily crop water stress index (CWSI) and cumulative irrigation application between 1 July and 15 September at each study site and study year.

Study Site	Parameter	Year			
		2017	2018	2019	2020
Vineyard-A	Daily CWSI	0.25	0.23	0.31	0.28
	Irrigation (mm)	66	130	117	122
Vineyard-B	Daily CWSI	0.38	0.44	0.41	0.36
	Irrigation (mm)	143	115	134	128

inches) (Fig. 3) and decreased the daily CWSI to near zero (Fig. 1). The estimated fASW increased on 18 August and 23 August (Fig. 4) as soil water contents increased (Fig 2) due to irrigation events. Prior to irrigation on 18 Aug, daily CWSI was greater than 0.6 (Fig. 1), while fASW for the 0 to 120 cm soil profile was about 0.3 and increased to greater than 0.8 following irrigation on 23 Aug. Midday on 25 August daily CWSI was near zero while fASW was about 0.78. An overnight irrigation

event started on 18 August is depicted as two irrigations since it spanned two days (Fig. 5). The first irrigation event applied about 10 mm (0.4 inch) and the second irrigation event applied about 21 mm (0.8 inch), which collectively decreased daily CWSI from 0.6 to near zero (Fig. 1) and increased fASW from 0.3 to 0.8 (Fig. 4).

The observed variability among radiometers on the irrigation DSS webpage for daily CWSI values (Fig. 1), was likely attributed to high spatial variability in soil profile characteristics. Limiting historical data on the irrigation DSS webpage to a running 12-day period was to optimize time efficiency of the user web browsing experience. The infield data logger that hosted the irrigation DSS webpages had limited computing capacity, so limiting the historical data time frame to a running 12-days offered a reasonable compromise between data viewability on a cell phone and time to transfer the data to the user webpage interface device. A running 12-day historical record was sufficient to establish trends in CWSI or soil water availability useful in making irrigation management decisions. The vineyard managers in this study

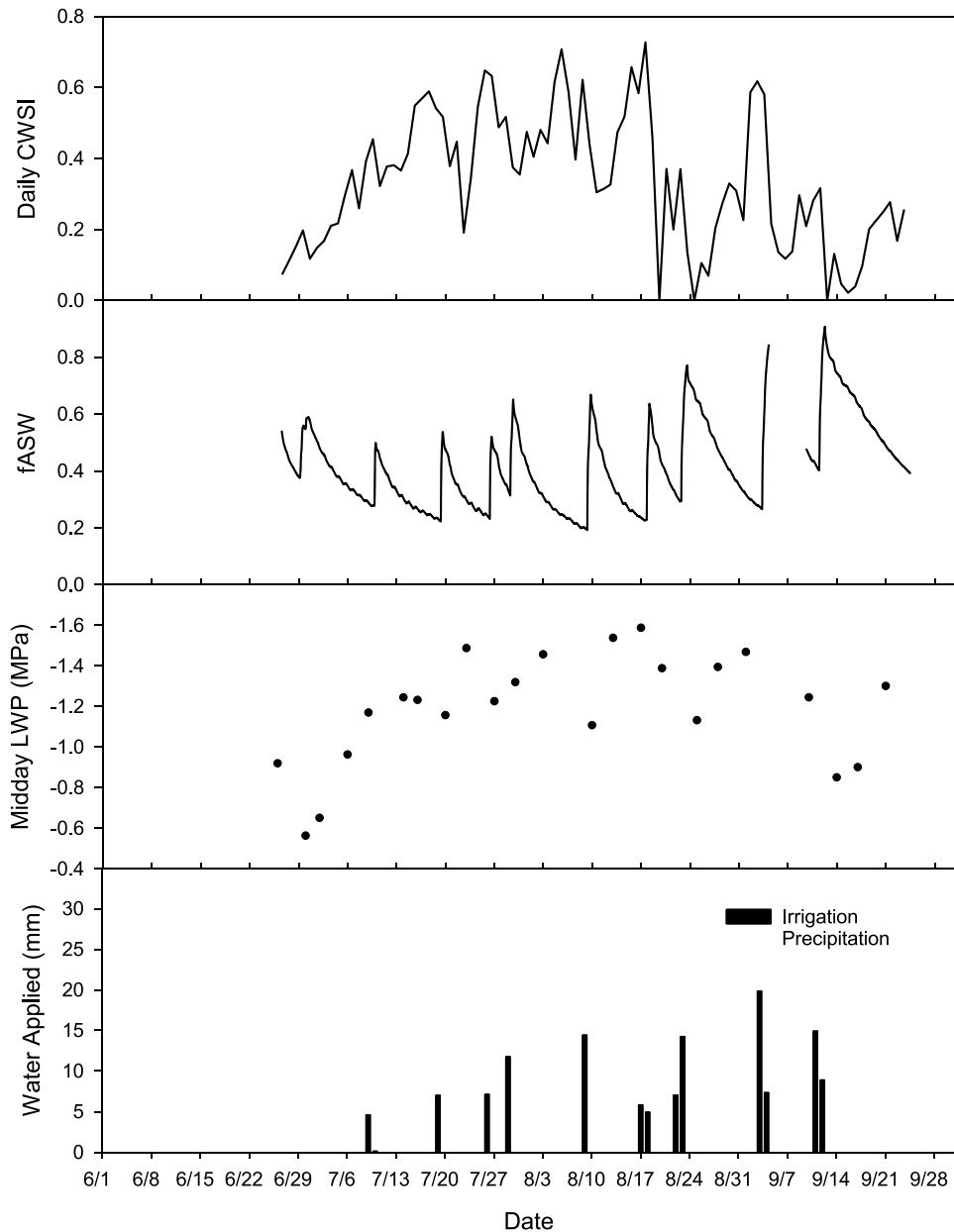


**Fig. 8.** Average daily CWSI, fraction of available soil water (fASW) in 0 to 120 cm soil profile, midday leaf water potential (LWP), precipitation, and irrigation during the 2020 growing season at V-B.

only wanted to know if they need to irrigation today and were largely uninterested in historical CWSI values. The 12-day historical length can be increased if deemed necessary by uploading the data to the cloud and using cloud based graphical software to display the same information for the full growing season.

#### 4.2. Relationship between measures of vine water status and irrigation

A seasonal graph of the irrigation DSS data for V-B in 2020 shows an interconnected response among the measured and estimated DSS parameters (Fig. 8). Values for daily CWSI and midday leaf water potential shown in Fig. 8 are averages of the measured values and fASW is for the 0 to 120 soil profile. Prior to initiation of measurements on 13 June, there was above average precipitation in 2020 (Table 1). The prior precipitation is evident by the status of well-watered vines on 13 June (Fig. 8). Daily CWSI was low, fASW was  $> 0.55$  and LWP was less negative. A rainfall event on 29 June was associated with a decrease in the daily CWSI, an increase in fASW and a less negative LWP. Prior to the irrigation event on 20 July, the daily CWSI steadily increased coincident with a more negative LWP. The small irrigation event on 8 July had minimal influence on daily CWSI or LWP potential as fASW remained below 0.55. Irrigation events prior to 17 August reduced CWSI and made LWP less negative for only a few days and fASW remained  $< 0.55$  for most of the duration. The seasonally highest CWSI values and most negative LWP values occurred between 28 July and 24 August. The irrigation event on 23 August and precipitation events on 17 and 24 August decreased CWSI to near zero, increased fASW to  $> 0.55$  and LWP became less negative, all of which indicated a short period of increase in vine water status. Between 24 August and the next irrigation event on 1 September, the CWSI increased, fASW decreased, and LWP became more negative. The relatively large ( $> 25$  mm) irrigation event on 3 September decreased daily CWSI to  $< 0.2$ , increased fASW to  $> 0.8$ , and LWP became less negative. The last irrigation on 11 September reduced daily CWSI to near zero, increased fASW to nearly 0.9 and increased LWP to  $> -0.9$  MPa.

The fASW is a common method used to express crop water stress for field crops. Wine grape is well-watered when fASW is greater than 0.55 [35]. The corresponding seasonal responses of fASW, midday LWP, and the daily CWSI to irrigation and precipitation events (Fig. 8) supports the usefulness and accuracy of daily CWSI for real-time irrigation management of wine grape irrespective of soil characteristics that may influence these values.

#### 4.3. Comparison of vine water stress measures between vineyards

The slopes of linear relationships between the fASW versus LWP or daily CWSI differed between vineyards (Fig. 7). This may be partially due to differences in soil textures and permeability between the vineyards. V-A had a silt loam soil with low to moderate permeability while V-B had a sandy soil with high permeability. Water applied by the drip irrigation emitter likely resulted in different wetting patterns between vineyards with a deeper wetting pattern and less lateral spreading at V-B. There was likely limited soil water availability outside the immediate area of the emitter wetting pattern at V-B due to the low water holding capacity of the sandy soil. The soil water sensor was installed within 20 cm of an emitter and may have provided a better measurement of total soil water at V-B than V-A. The greater water holding capacity of the silt loam soil at V-A likely resulted in much more stored soil water from non-growing season precipitation, limiting the range in fASW over the growing season. However, the range in LWP were similar between vineyards. The low permeability of the soil at V-A may have restricted movement of soil water to the roots. Lastly the soil at V-A exhibited silica cementation ranging from 45 to 60 cm deep during soil sensor installation that may have restricted root growth. Ample soil water was measured below 60 cm in the root zone (data not shown) but very little extraction occurred during the growing season supporting the suspicion

of limited root presence below 60 cm. The presence of ample soil water below 60 cm limited the range in fASW over the growing season and if it was largely unavailable to the vines would result in high daily CWSI and low LWP values despite fASW  $> 0.55$ .

Despite a significant linear relationship between daily CWSI and midday LWP for both vineyards (Fig. 7), there is considerable variability in the relationships, which precludes use of CWSI as a direct surrogate for LWP. A quadratic relationship between CWSI and LWP averaged over four wine grape cultivars was reported by [21], which depicted a similar degree of variability. [36] reported LWP ranging from  $-0.51$  to  $-1.15$  MPa for well-watered grapevines in California with LWP linearly related to vapor pressure deficit (VPD) and  $T_a$ . They also reported a linear relationship between LWP and VPD for water stressed vines, but with reduced dependence on VPD compared to well-watered vines. The results of this study are consistent with the findings of [36] as the relationship between CWSI and LWP (Fig. 7) could be represented by a piece-wise linear relationship with CWSI  $\approx 0$  for LWP  $> -1.15$  MPa. Solar radiation also influences LWP and LWP measurements should be collected on cloudless days [36]. The LWP values reported in this study were made over a wide range of VPD and on days with variable clouds. Additionally, some LWP values reported in this study were not collected on the same vine used for canopy temperature measurement, another source of variability in the relationship between CWSI and LWP. Overall, the presence of water stress detected by LWP measurement was also indicated by daily CWSI as calculated in this study, demonstrating that CWSI can be effectively used as an irrigation management tool for wine grape. The vineyard managers in this study were successful in using daily CWSI to achieve similar levels of plant water stress over multiple years, despite yearly differences in evaporative demand and growing season precipitation. The primary advantage of using CWSI as an irrigation management tool is the ability to automate data collection for daily monitoring of water stress with minimal labor.

The linear relationship between fASW and daily CWSI exhibited less variability than the linear relationship between fASW and midday LWP (Fig. 7), especially for V-B. Thus, CWSI was a more direct indicator of available soil water than LWP. For V-B, when fASW was  $> 0.55$ , indicating well-watered vines, CWSI was  $< 0.1$  supporting the rational that CWSI should approach zero for well-watered vines and approach one for severely watered stressed vines as the linear relationship depicts. However, for V-A a fASW value of 0.55 corresponds to a CWSI value  $> 0.5$ , which clearly does not follow the rational of CWSI, indicating an error in estimating fASW. As forementioned, this discrepancy is likely due to the effective root zone of the vines less than the 120 cm depth used to compute fASW. The estimates of FC and PWP of the soil at V-A could also be in error, which could lead to overestimation of fASW. If estimates of the fASW at V-A were reduced by 25%, a fASW value of 0.55 would correspond to a CWSI value  $< 0.1$ , like V-B and a CWSI value of 0.6 would correspond to a fASW of 0.37. The unrealistic over estimation of fAWC at V-A based on measured midday LWP and calculated daily CWSI highlights the difficulty in accurately quantifying the fASW using a single soil moisture profile measurement with drip irrigated crops. Drip irrigation results in a 3-dimensional wetting pattern that makes reliable estimation of root zone available soil water difficult at best. As an example, [37] reported that nine neutron probe measurements in one quadrant of a vine root zone, to a depth of 3 m, was necessary to quantify soil water content of drip-irrigated grape vines. The difficulty in quantifying fASW in drip irrigated vineyards highlights the advantage of using plant-based methods for assessing vine water status such as CWSI provided the reference temperatures  $T_{LL}$  and  $T_{UL}$  can be reliably estimated.

#### 4.4. Seasonal CWSI and seasonal irrigation amounts between vineyard managers

Neither vineyard manager in this study used any type of quantitative plant or soil water monitoring techniques to aid in irrigation



management decisions prior to the installation of the CWSI based IoT irrigation DSS. Prior to this study, the irrigation managers at both vineyards made irrigation decisions based upon intuition, previous experience, and crop appearance [1]; so, there was a reasonable expectation that the vineyard managers would actively use the CWSI based IoT irrigation DSS. At the beginning of the first study year, the vineyard managers were briefed on the concept of CWSI for monitoring plant water status and were given the guideline that a daily CWSI value of 0.3 corresponded to approximately a 70% ET rate relative to a well-watered, 100% ET. Beyond that initial guidance on how to interpret the daily CWSI value, the vineyard managers independently accessed the irrigation DSS webpages and made irrigation management decisions without input from research project personnel. At the end of the first study year both vineyard managers reported that they routinely accessed the irrigation DSS webpages for daily CWSI and fASW and used the information to support irrigation management decisions. In each of the remaining three years of the study, both vineyard managers, at their discretion, continued to access the irrigation DSS webpages and use the daily CWSI to facilitate irrigation management decisions.

Seasonal average daily CWSI values (Table 2) were higher for V-B as the vineyard manager preferred higher plant water stress than the manager of V-A. The higher daily CWSI value at V-B was also higher because it would rapidly increase a couple days after an irrigation event due to the low water holding capacity of the sandy soil. Cumulative irrigation water application was surprisingly similar across vineyards, particularly for years 2018 through 2020, despite differences in soil water holding capacity and vineyard managers. Cumulative irrigation was low in the first year of the study at V-A due to above average non-growing season precipitation and higher water holding capacity of the silt loam soil. The narrow range in seasonal average daily CWSI (0.23 to 0.31 for V-A, and 0.36 to 0.44 for V-B) and cumulative irrigation (1.14 to 134 mm) in 2018 through 2020 suggests that vineyard managers effectively used the CWSI based IoT irrigation DSS to develop and maintain a consistent deficit irrigation management program.

#### 4.5. Irrigation decision support system limitations

The data-driven models used in this study provided reliable estimates of  $T_{LL}$  and  $T_{UL}$  in real-time for the semiarid climatic conditions of the study site, which was representative of the irrigated wine producing locations in the Pacific Northwest U.S. The climatic conditions under which these data-driven models were developed were representative of the conditions in this study. However, the models may not perform as well in other regions with weather conditions outside the database range for model development. For example, in areas where daily windspeeds exceed  $5 \text{ m sec}^{-1}$ . Wind speeds higher than  $5 \text{ m sec}^{-1}$  were not included in the database used for model development and grapevines are known to reduce stomatal conductance under high winds [38,39]. A wind induced reduction in stomatal conductance would result in an increase in canopy temperature independent of plant water stress and, since the data-driven model estimate of  $T_{LL}$  would be too low, the calculated CWSI value would be elevated. Canopy temperature data for well-watered vines under high wind conditions would need to be included in the data set used to calibrate the neural network model for estimating  $T_{LL}$  in windy semiarid regions.

There are climatic conditions that can result in a calculated CWSI value of less than zero or greater than one. Wet canopy conditions typically result in measured canopy temperature that is less than the  $T_{LL}$  predicted by the data driven model. This results in a negative CWSI value regardless of soil water availability. The original development of the CWSI concept by [15] was limited to clear sunny conditions. However, the data driven model for predicting  $T_{LL}$  that was used in this study uses a database of well-watered vine canopy temperatures that were measured under variable cloudy conditions. The data driven model can therefore predict  $T_{LL}$  for variably cloudy conditions. While the data-driven model used for predicting  $T_{LL}$  is valid for solar radiation <

$100 \text{ W m}^{-2}$ ,  $T_{UL}$  predicted using Eq. (2) for low levels of solar radiation can be approximately equal to  $T_{LL}$  resulting in CWSI values less than zero or greater than 1. In this study, solar radiation less than  $200 \text{ W m}^{-2}$  often resulted in CWSI values less than zero. [40] also found solar radiation greater than  $200 \text{ W m}^{-2}$  was necessary to reliably use canopy temperature measurement for irrigation scheduling. In this study, daily CWSI was limited to a maximum of one and a minimum of zero in software to avert illogical values. The effect of wet canopy and low solar radiation on calculation of daily CWSI is evident in Fig. 8 on 18 and 24 August when a value of zero was assigned to daily CWSI during rainfall events. Limiting daily CWSI value to zero due to low solar radiation or wet canopy has little practical impact on use of CWSI for irrigation management as vine water stress is low under these circumstances due to low evaporative demand. When calculated CWSI is greater than one due to low solar radiation, limiting the value of one is more problematic as this results in a very erroneous representation of vine water stress that could lead to an unnecessary irrigation event.

The climatic conditions leading to errors in calculating CWSI (rainfall, low solar radiation) are limited to 1-to-3-days in duration in the semiarid regions of the Pacific Northwest U.S. and do not prevent application of the CWSI based IoT irrigation DSS system in the region. Software used to compute CWSI can be modified to detect these events and indicate to the user that the daily CWSI is unavailable. The daily CWSI value for the day preceding the rainfall or low solar radiation event can be used to guide irrigation decisions as plant water stress will decrease with rainfall or increase minimally as ET will be small under low solar radiation conditions.

The CWSI based IoT irrigation DSS system developed and implemented in this study focused on two small acreage, commercial estate vineyards in semiarid southwestern Idaho USA. The climatic conditions at the study sites were representative of vineyards in the semiarid irrigated regions of the Pacific Northwest U.S. Small acreage vineyards can be found throughout the region and most do not have staff with irrigation science training, nor can they afford to hire trained vineyard irrigation management professionals or services. They need affordable irrigation scheduling tools that are easy to maintain and indicate when to irrigate to maintain a desired level of vine water stress. The vineyard managers at the study sites were pleased the system reliably and timely indication of vine water stress without having to spend time collecting soil water content measurements needed to estimate fASW or measure leaf water potential. While this study focused on small commercial estate vineyards, the IoT irrigation DSS concept is applicable to larger commercial vineyards where it could be used to provide plant water stress information needed to ground truth remote sensing based estimates of the ratio of actual-to-reference ET such as those provided by GRAPEX [41] or OPENET (<https://openetdata.org>). These remote sensing-based estimates have a minimum spatial resolution of 30 m, which is larger than the minimum dimension of irrigation management blocks in many commercial estate vineyards, hence they are not necessarily applicable to small commercial estate vineyards in the region.

The CWSI based IoT irrigation DSS system implemented in this study used expensive scientific grade equipment, which proved invaluable to investigate the validity and adoptability of the system for irrigation management in wine grapes. The infrared temperature sensors cost \$700 each, the multifunctional precision data logger was \$2000, and the cellular modem with accessories was \$700 totaling over \$6100 excluding web page publishing software and climatic sensors. The soil moisture sensor cost is not included as it is unnecessary for calculation of the CWSI. The cost of the equipment used in this study is prohibitive for small vineyards to monitor just a single location.

Vineyard manager acceptance and adoption of the CWSI based IoT irrigation DSS system implemented in this study justifies continued development and enhancement of the system. Future work will focus on incorporating less expensive infrared temperature sensors coupled with low-power, low-cost radio communications to allow wireless transfer of

data to a base station. The base station will be connected to the internet using a cell phone modem and used to upload canopy temperature measurements across a vineyard to a cloud computing platform. The cloud computing platform software will be used to host webpages like those used in this project to allow real-time monitoring of canopy temperature at sensor locations across a vineyard and display daily CWSI for each canopy temperature monitoring location. These system enhancements would increase size of the vineyard area represented by daily CWSI measurements, encompassing multiple cultivars and irrigation blocks or irrigation management zones in larger vineyards.

## 5. Conclusions

A CWSI based IoT irrigation DSS was developed, and field tested at two small acreage commercial wine grape estate vineyards in south-western Idaho. Irrigation DSS webpages, accessible to vineyard managers via cell phone or computer, provided a running 12-day history of CWSI daily values, soil moisture and current weather conditions. Data-driven models were used to estimate reference temperatures needed to calculate the CWSI using real-time environmental inputs for  $R_s$ ,  $T_a$ ,  $RH$ , and  $WS$ . Edge computing on a solar powered, field-deployed data logger was used to calculate the CWSI and fASW, and the data logger was used to host webpages of the irrigation DSS. The data logger was connected to a cellular modem located in the vineyard. The vineyard managers routinely used the irrigation DSS webpage for the CWSI and soil moisture to make irrigation management decisions. The average daily CWSI and irrigation amounts between 1 July and 15 September were similar between years over the four-year study for each study vineyard suggesting that the CWSI based IoT irrigation DSS was effective in assisting irrigation management decisions.

Linear relationships between daily CWSI, midday LWP, and fraction of available soil water were significant ( $p < 0.001$ ) at both study sites. The coefficient of determination ( $R^2 = 0.58$ ) for the linear relationship between daily CWSI and fraction of available soil water for V-B was better than that for midday LWP ( $R^2 = 0.38$ ) indicating daily CWSI was the most reliable indicator (less variable) of vine water status.

The data-driven models used to estimate  $T_{LL}$  and  $T_{UL}$  can result in CWSI values outside the theoretical range of 0 to 1 when the canopy is wet from precipitation or solar radiation is  $<200 \text{ W m}^{-2}$ . These climatic conditions are limited to 1-to-3-days in duration in the semiarid regions of the Pacific Northwestern U.S. and do not prevent application of the CWSI based IoT irrigation DSS system in the region. These climatic instances can be detected by IoT irrigation DSS system software and indicate to the user that the daily CWSI is unavailable. The daily CWSI value for the day preceding the rainfall or low solar radiation event can be used to indicate plant water stress since it will decrease with rainfall or increase minimally as ET will be small under low solar radiation conditions.

The hardware and software used to implement the CWSI based IoT irrigation DSS in this study was very reliable but too expensive for practical commercial application. Future work will focus on incorporating less expensive infrared temperature sensors coupled with low-power, low-cost radio communications to allow wireless transfer of data to a base station. The base station will be connected to the internet using a cell phone modem and upload canopy temperature measurements across a vineyard to a cloud computing platform. The cloud computing platform software will be used to host webpages like those used in this project to allow real-time monitoring of canopy temperature at sensor locations across a vineyard and display daily CWSI for each canopy temperature monitoring location.

## Funding

The work reported in this paper was partially funded by the Idaho Department of Agriculture 2014 Idaho Specialty Crop Block Grant #2014-14-SCBG-ID-0016 and the Idaho Department of Agriculture 2016

Idaho Specialty Crop Block Grant #2016-16SCBGID0034.

## Declaration of Competing Interest

The authors declare that they have no known competing financial interests or personal relationships that could have appeared to influence the work reported in this manuscript.

## Data availability

Data will be made available on request.

## Acknowledgment

The authors thank Alan Muir, USDA-ARS Horticultural Crops Research Unit, for providing technical support for field management, sensor installation, sample collection and analysis. The authors also thank the cooperating vineyard owners for their active participation in the reported research.

## References

- [1] M. Moyer, R.T. Peters, R. Hamman, *Irrigation Basics for Eastern Washington vineyards*, Washington State University Extension, Pullman, WA, 2013, p. 12.
- [2] M.M. Chaves, et al., Grapevine under deficit irrigation: hints from physiological and molecular data, *Ann. Bot.* 105 (2010) 661–676, <https://doi.org/10.1093/aob/mcq030>.
- [3] M.M. Chaves, et al., Deficit irrigation in grapevine improves water-use efficiency while controlling vigour and production quality, *Ann. Appl. Biol.* 150 (2007) 237–252, <https://doi.org/10.1111/j.1744-7348.2006.00123.x>.
- [4] E. Fereres, M.A. Soriano, Deficit irrigation for reducing agricultural water use, *J. Exp. Bot.* 58 (2006) 147–159, <https://doi.org/10.1093/jxb/erl165>.
- [5] K.C. Shellie, Water productivity, yield, and berry composition in sustained versus regulated deficit irrigation of Merlot grapevines, *Am. J. Enol. Vitic.* 65 (2014) 197–205, <https://doi.org/10.5344/ajev.2014.13112>.
- [6] A.P. Williams, B.I. Cook, J.E. Smerdon, Rapid intensification of the emerging southwestern North American megadrought in 2020–2021, *Nat. Clim. Chang.* (2022), <https://doi.org/10.1038/s41558-022-01290-z>.
- [7] J.M. Mirás-Avalos, E.S. Araujo, Optimization of vineyard water management: challenges, strategies, and perspectives, *Water* 13 (2021) 746, <https://doi.org/10.3390/w13060746>.
- [8] M. Rienth, T. Scholasch, State-of-the-art of tools and methods to assess vine water status, *OENO One* 53 (2019), <https://doi.org/10.20870/oeno-one.2019.53.4.2403>.
- [9] J.E. Fernández, Plant-based methods for irrigation scheduling of woody crops, *Horticulturae* 3 (2017) 35, <https://doi.org/10.3390/horticulturae3020035>.
- [10] A.D. Levin, Re-evaluating pressure chamber methods of water status determination in field-grown grapevine (*Vitis* spp.), *Agric. Water Manag.* 221 (2019) 422–429, <https://doi.org/10.1016/j.agwat.2019.03.026>.
- [11] K. Raschke, Heat transfer between the plant and the environment, *Annu. Rev. Plant Physiol.* 11 (1960) 111–126, <https://doi.org/10.1146/annurev.pp.11.060160.000551>.
- [12] C.B. Tanner, Plant temperatures, *Agron. J.* 55 (1963) 210–211, <https://doi.org/10.2134/agronj1963.00021962005500020043x>.
- [13] J.L. Hatfield, The utilization of thermal infrared radiation measurements from grain sorghum crops as a method of assessing their irrigation requirements, *Irrig. Sci.* 3 (1983) 259–268, <https://doi.org/10.1007/BF00272841>.
- [14] R.D. Jackson, et al., Canopy temperature as a crop water stress indicator, *Water Resour. Res.* 17 (1981) 1133–1138, <https://doi.org/10.1029/WR017i004p01133>.
- [15] S.B. Idso, et al., Normalizing the stress-degree-day parameter for environmental variability, *Agric. Meteorol.* 24 (1981) 45–55, [https://doi.org/10.1016/0002-1571\(81\)90032-7](https://doi.org/10.1016/0002-1571(81)90032-7).
- [16] Y. Cohen, et al., Estimation of leaf water potential by thermal imagery and spatial analysis, *J. Exp. Bot.* 56 (2005) 1843–1852, <https://doi.org/10.1093/jxb/eri174>.
- [17] D.M. Glenn, et al., Impact of kaolin particle film and water deficit on wine grape water use efficiency and plant water relations, *HortScience* 45 (2010) 1178–1187, <https://doi.org/10.21273/hortsci.45.8.1178>.
- [18] K.C. Shellie, B.A. King, Kaolin particle film and water deficit influence malbec leaf and berry temperature, pigments, and photosynthesis, *Am. J. Enol. Vitic.* 64 (2013) 223–230, <https://doi.org/10.5344/ajev.2012.12115>.
- [19] K.C. Shellie, B.A. King, Application of a daily crop water stress index to deficit irrigate malbec grapevine under semi-arid conditions, *Agriculture* 10 (2020) 492, <https://doi.org/10.3390/agriculture10110492>.
- [20] J. Bellvert, et al., Mapping crop water stress index in a 'Pinot-noir' vineyard: comparing ground measurements with thermal remote sensing imagery from an unmanned aerial vehicle, *Precis. Agric.* 15 (2014) 361–376, <https://doi.org/10.1007/s11119-013-9334-5>.

- [21] J. Bellvert, et al., Seasonal evolution of crop water stress index in grapevine varieties determined with high-resolution remote sensing thermal imagery, *Irrig. Sci.* 33 (2015) 81–93, <https://doi.org/10.1007/s00271-014-0456-y>.
- [22] E.J. Sadler, et al., Corn canopy temperatures measured with a moving infrared thermometer array, *Trans. ASAE* 45 (2002) 581, <https://doi.org/10.13031/2013.8855>.
- [23] J.R. Mahan, K.M. Yeater, Agricultural applications of a low-cost infrared thermometer, *Comput. Electron. Agric.* 64 (2008) 262–267, <https://doi.org/10.1016/j.compag.2008.05.017>.
- [24] V. Alchanatis, et al., Evaluation of different approaches for estimating and mapping crop water status in cotton with thermal imaging, *Precis. Agric.* 11 (2010) 27–41, <https://doi.org/10.1007/s11119-009-9111-7>.
- [25] H.G. Jones, Use of infrared thermometry for estimation of stomatal conductance as a possible aid to irrigation scheduling, *Agric. For. Meteorol.* 95 (1999) 139–149, [https://doi.org/10.1016/S0168-1923\(99\)00030-1](https://doi.org/10.1016/S0168-1923(99)00030-1).
- [26] H.G. Jones, *Plants and Microclimate: a Quantitative Approach to Environmental Plant Physiology*, Cambridge University Press, Cambridge, 2013, 3 ed.
- [27] I. Leinonen, H.G. Jones, Combining thermal and visible imagery for estimating canopy temperature and identifying plant stress, *J. Exp. Bot.* 55 (2004) 1423–1431, <https://doi.org/10.1093/jxb/erh146>.
- [28] S.A. O'Shaughnessy, et al., Using radiation thermography and thermometry to evaluate crop water stress in soybean and cotton, *Agric. Water Manag.* 98 (2011) 1523–1535, <https://doi.org/10.1016/j.agwat.2011.05.005>.
- [29] A. Pou, et al., Validation of thermal indices for water status identification in grapevine, *Agric. Water Manag.* 134 (2014) 60–72, <https://doi.org/10.1016/j.agwat.2013.11.010>.
- [30] J.C. O'Toole, J.G. Real, Estimation of aerodynamic and crop resistances from canopy temperature, *Agron. J.* 78 (1986) 305–310, <https://doi.org/10.2134/agronj1986.00021962007800020019x>.
- [31] J.O. Payero, S. Irmak, Variable upper and lower crop water stress index baselines for corn and soybean, *Irrig. Sci.* 25 (2006) 21–32, <https://doi.org/10.1007/s00271-006-0031-2>.
- [32] B.A. King, K.C. Shellie, Evaluation of neural network modeling to predict non-water-stressed leaf temperature in wine grape for calculation of crop water stress index, *Agric. Water Manag.* 167 (2016) 38–52, <https://doi.org/10.1016/j.agwat.2015.12.009>.
- [33] B.A. King, et al., Data-driven models for canopy temperature-based irrigation scheduling, *Trans. ASABE* 63 (2020) 1579–1592, <https://doi.org/10.13031/trans.13901>.
- [34] K.C. Shellie, Vine and berry response of Merlot (*Vitis vinifera* L.) to differential water stress, *Am. J. Enol. Vitic.* 57 (2006) 514–518.
- [35] Allen, R.G., et al., *Crop evapotranspiration: guidelines for computing crop water requirements*, *FAO Irrigation and Drainage Paper #56*, 1998, Rome, Italy: FAO.
- [36] L.E. Williams, P. Baeza, Relationships among ambient temperature and vapor pressure deficit and leaf and stem water potentials of fully irrigated, field-grown grapevines, *Am. J. Enol. Vitic.* 58 (2007) 173–181.
- [37] L.E. Williams, T.J. Trout, Relationships among vine- and soil-based measures of water status in a thompson seedless vineyard in response to high-frequency drip irrigation, *Am. J. Enol. Vitic.* 56 (2005) 357–366.
- [38] J.M. Kobriger, W.M. Kliewer, S.T. Lagier, Effects of wind on water relations of several grapevine cultivars, *Am. J. Enol. Vitic.* 35 (1984) 164–169.
- [39] J.M. Campbell-Clause, Stomatal response of grapevines to wind, *Aust. J. Exp. Agric.* 38 (1998) 77–82, <https://doi.org/10.1071/EA91220>.
- [40] D.L. Bockhold, et al., Irrigation scheduling based on crop canopy temperature for humid environments, *Trans. ASABE* 54 (2011) 2021–2028, <https://doi.org/10.13031/2013.40654>.
- [41] K.R. Knipper, et al., Evapotranspiration estimates derived using thermal-based satellite remote sensing and data fusion for irrigation management in California vineyards, *Irrig. Sci.* 37 (2019) 431–449, <https://doi.org/10.1007/s00271-018-0591-y>.